World Academy of Science, Engineering and Technology
International Journal of Mechanical and Mechatronics Engineering
Vol:7, No:7, 2013

A Study on Characteristics and Geometric Parameters of the Flat Porous Aerostatic Bearing

T. Y. Huang, B. Z. Wang, S. C. Lin, and S. Y. Hsu

***Abstract*—**A CFD software was employed to analyze the characteristics of the flat round porous aerostatic bearings. The effects of gap between the bearing and the guide way and the porosity of the porous material on the load capacity of the bearing were studied. The adequacy of the simulation model and the approach was verified. From the parametric study, it is found that the depth of the flow path does not influence the load capacity of the bearing; the load capacity of the bearing will decrease if the thickness of the porous material increases or the porous material protrudes above the bearing housing; the variation of the chamfer at the edge of the bearing does not affect the bearing load capacity. For a bearing with an air gap of 5μm and a porosity of 0.1, the average load capacity and the pressure distribution of the bearing are nearly unchanged no matter the bearing moves at a constant or a varying speed.

***Keywords*—**Aerostatic bearing, Load capacity, Porosity, Porous material.

I. Introduction

THE use of the porous material as the restrictor in aerostatic bearings has many advantages over the conventional orifice restrictors such as simplicity of design and manufacture, higher load capacity and stiffness and good stability at high operational speed. With broad applications in different fields, the porous aerostatic bearings attract attentions from various industries. The static and dynamic characteristics of porous aerostatic bearings have been studied extensively, both theoretically and experimentally. Thrust bearings are by far the simplest geometry for theoretical analyses, and are therefore the most widely reported.

Assuming the laminar and incompressible flow obeys Darcy's law, Sheinberg and Shuster [1] reported theoretical analyses of the pressure distribution, load capacity and gas consumption of the porous aerostatic thrust bearings. Gargiulo and Gilmour [2] used the finite difference method to analyze the characteristics of the thrust bearings including provision for compressibility of the lubricant and anisotropic permeability of the porous media. Andrisano and Maggiore [3] did numerical analysis on the effects of bearing tilt and surface roughness with correction to the bearing gap. They also did experiment on load capacity and gas consumption. Ishizawa and Hori [4] were the pioneers to study the effect of velocity slip at the porous bearing surface. Beavers and Joseph [5] proposed a theory based on replacing the effect of the boundary layer with a slip velocity proportional to the exterior velocity gradient and verified it by experiment. Based on the Beavers and Joseph model, Murti [6] analyzed the porous thrust pad externally pressurized with an incompressible fluid with slip flow at the porous boundary. Assuming the flow in the bearing matrix is predominantly axial, Verma [7] obtained modified expressions for the characteristics of an externally pressurized circular porous thrust bearing by using the appropriate conditions given by Beavers and Joseph. Hsing [8] indicated that, for small value of film thickness commonly used in aerostatic bearings, the inertia effect is confined to a narrow region near the edge of the bearing, with little influence on load capacity and stiffness. Taylor and Lewis [9] investigated the change in bearing-gap geometry due to elastic deformation of the porous pad under working pressure. They assumed a perfectly flat pad under no load, resulting in a diverging gap when pressure was applied and leading to a reduction in pressure.

Rao [10], [11], Singh and Rao [12]–[14], Singh et al. [15]–[17] employed the finite difference method to solve the modified Reynolds equation derived from the Navier–Stokes equations using the Beavers–Joseph slip velocity condition at the porous interface for studying the effects of offset loads [10]–[13], velocity slip [11]–[15], bearing tilt [12]–[14], and combination of velocity slip, permeability anisotropy and bearing tilt [16]–[17] on the characteristics of porous aerostatic rectangular and annular thrust bearings. The pressure distribution, the load capacity, the mass flow rate and the static stiffness were computed for various operating conditions. Koyama et al. [18] studied the effects of anisotropic permeability, porosity and thickness of porous-ceramics materials on the stiffness, load carrying capacity and pneumatic instability of the porous-ceramics air bearings by the finite element method and experiment. They pointed out that the porosity and thickness of the porous materials should be kept as small as possible to obtain higher stiffness and stability. Tian [19] presented a modified three-dimensional flow model deduced from the Darcy equation and the modified Reynolds equation and used the finite element method to calculate the pressures in the gas film and porous matrix. Kwan and Corbett [20] reported that velocity slip at the porous surface did not obey the Beavers model, but could be approximated by an added equivalent clearance. They used an equivalent clearance method, in conjunction with a proposed approximation to correct for inertia effects, to modify the simple one-dimensional model. Yoshimoto and Kohno [21] studied the static and dynamic characteristics of aerostatic circular

T. Y. Huang is professor with the Mechanical Engineering Department, Lunghwa University of Science and Technology, Taoyuan, Taiwan. (phone: 886-2-8209-3211; fax: 886-2-8209-6865; e-mail: tyhuang@ mail.lhu.edu.tw).

B. Z. Wang and S. C. Lin are with the Mechanical Engineering Dept., National Taiwan University of Science and Technology, Taipei, Taiwan.

S. Y. Hsu is a senior project engineer with the Mechanical and Systems Research Laboratories, Industrial Technology Research Institute, Hsinchu, Taiwan.

porous thrust bearing with the air supplied by the annular groove or the hole. Luong et al. [22] applied the finite element method to predict the performance of aerostatic thrust bearings with a complete porous surface. Their model including unflatness and deformation of the bearing surface correlated well with the experimental results. Miyatake et al. [23] investigated the static and dynamic characteristics of the aerostatic porous thrust bearings with a deep feed groove. Wu and Tao [24] applied the CFD code, FLUENT, to analyze the static characteristics of porous aerostatic thrust bearings.

II. Fundamentals and Approaches

Based on the finite volume method and the pressure-velocity coupling scheme of the SIMPLE algorithm with the standard *k-ε* turbulence model, this study utilized the software, FLUENT, to solve the incompressible three dimensional Navier-Stokes equations to study the flow field of a porous aerostatic bearing for its physical behaviors such as velocity and pressure. Due to uncertainty of the porosity of the porous material, different magnitudes of the porosity are assumed for analyzing the velocity, the pressure and the load capacity of the bearing with different design parameters. The computed results of the load capacity are compared with the experimental data shown in the product specifications published by New Way Company to evaluate the adequacy of the used approach and the assumed porosity. The governing equations, the turbulent model and the boundary conditions considered in the analysis are introduced in the following sections:

A. Governing Equation and Turbulent Model

For the purpose of numerical simulation, the flow field was simplified by the following assumptions:

1. The speed of flow in the bearing is fairly slow. Hence the air flow can be assumed to be incompressible and steady in all three dimensions.
2. The air is assumed to be a Newtonian flow with an invariant density. The gravity and the heat radiation effects are neglected. The viscosity of the air is a constant.
3. All physical properties are independent of the temperature. The ambient temperature is a constant.

The continuity and the momentum equations in conservative form are expressed as follows.

Continuity equation:

$$\frac{\partial u_i}{\partial x_i} = S_m \tag{1}$$

where x_i is the coordinate direction, u_i is the velocity tensor and S_m is the source term.

Momentum equation:

$$\rho\frac{\partial u_i}{\partial t} + \rho\frac{\partial (u_i u_j)}{\partial x_j} = -\frac{\partial p}{\partial x_i} + \frac{\partial}{\partial x_j}[\mu(\frac{\partial u_i}{\partial x_j} + \frac{\partial u_j}{\partial x_i})] + \rho g_i + F_i \tag{2}$$

where ρ is the fluid density, μ is the dynamic viscosity, g_i is the gravity and F_i is the body force.

When the fluid inertia affects the flow field more significantly than the fluid viscosity, the flow develops into a turbulent flow. The *k-ε* equation for turbulence proposed by Launder and Spalding [25] is employed to solve the Navier-Stokes equations.

$$\begin{aligned}&\frac{\partial}{\partial t}(\rho u_i) + \frac{\partial}{\partial x_j}(\rho u_i u_j) \\ &= -\frac{\partial p}{\partial x_i} + \frac{\partial}{\partial x_j}[\mu(\frac{\partial u_i}{\partial x_j} + \frac{\partial u_j}{\partial x_i} - \frac{2}{3}\delta_{ij}\frac{\partial u_i}{\partial x_i})] \\ &+ \frac{\partial}{\partial x_j}(-\rho\overline{u_i' u_j'})\end{aligned} \tag{3}$$

where the Reynolds stresses are modeled employing the Boussinesq hypothesis [26].

$$-\rho\overline{u_i' u_j'} = \mu_t(\frac{\partial u_i}{\partial x_j} + \frac{\partial u_j}{\partial x_i}) - \frac{2}{3}(\rho k + \mu_t\frac{\partial u_i}{\partial x_i})\delta_{ij} \tag{4}$$

There are two important turbulent parameters associated with the *k-ε* turbulent model, namely the turbulent kinetic energy *k* and the turbulent dissipation rate *ε*. The turbulent kinetic energy equation is in the form as

$$\begin{aligned}\frac{\partial}{\partial t}(\rho k) + \frac{\partial}{\partial x_i}(\rho k u_i) = \frac{\partial}{\partial x_j}\left[(\mu + \frac{\mu_t}{\sigma_k})\frac{\partial k}{\partial x_j}\right] \\ + G_k + G_b - \rho\varepsilon - Y_M + S_k\end{aligned} \tag{5}$$

The turbulent dissipation rate equation is in the form as

$$\begin{aligned}\frac{\partial}{\partial t}(\rho\varepsilon) + \frac{\partial}{\partial x_i}(\rho\varepsilon u_i) = \frac{\partial}{\partial x_j}\left[(\mu + \frac{\mu_t}{\sigma_\varepsilon})\frac{\partial \varepsilon}{\partial x_j}\right] \\ + C_{1\varepsilon}\frac{\varepsilon}{k}(G_k + C_{3\varepsilon}G_b) - C_{2\varepsilon}\rho\frac{\varepsilon^2}{k} + S_\varepsilon\end{aligned} \tag{6}$$

where σ_k and σ_ε are the turbulent Prandtl coefficients in the turbulent kinetic energy equation and the turbulent dissipation rate equation, respectively. G_k and G_b are the turbulent kinetic energies generated by the mean velocity gradients and the buoyancy, respectively. S_k and S_ε are the momentum source terms. Y_M represents the contribution of the fluctuating dilatation in compressible turbulence to the overall dissipation rate, and $C_{1\varepsilon}$, $C_{2\varepsilon}$, $C_{3\varepsilon}$ and C_μ are model constants [25]. The turbulent viscosity μ_t is defined as a function of *k* and *ε* in the following form.

$$\mu_t = \rho C_\mu (k^2/\varepsilon) \quad (7)$$

B. Boundary Conditions

1. Inlet boundary condition: The air is pumped into the bearing at 4atm (410 kPa).
2. Outlet boundary condition: The air is discharged from the bearing to the ambient atmosphere at 1atm (102.5 kPa).
3. Wall function: The flow passing by the solid wall must meet not only the no-penetration condition, but also the no-slip condition. On selection of the standard $k-\varepsilon$ turbulent model, the wall function in the option of Near-Wall Treatment has to be employed.
4. Slip wall boundary condition: It is assumed that the surface of the porous material is under slip wall boundary condition, and the rest solid surface is under no-slip condition. Regarding the slip flow, Beavers and Joseph proposed the following equation:

$$\partial u(x,0^+)/\partial y = \alpha[u(x,0^+) - u_p]/\sqrt{K} \quad (8)$$

where u_D is the uniform Darcy velocity, K is the permeability coefficient of the porous material, α is the dimensionless slip coefficient with a value between 0.01 and 5 depending on the material. Based on the theory of Beavers and Joseph [5], the permeability coefficient is defined in FLUENT software to deal with the slip wall boundary condition.

5. Moving wall boundary condition: The moving wall boundary condition is defined for the bottom surface of the bearing next to the air gap.

III. Simulation Model and Techniques

Numerical simulation was performed to analyze the characteristics of the carbon type S1012501 flat round porous aerostatic bearing (Fig. 1) made by New Way Inc. The round graphite plate above the concentric circular air flow grooves is the porous medium with a diameter of 123mm and a thickness of 3.5mm inside the aluminum housing and protrusion of 1mm from the housing

Due to axi-symmetry in shape, only a quarter of the flat round porous aerostatic bearing is modeled. The inlet of air in the bearing is not included to further simplify the geometry of the three dimensional model as is shown in Fig. 2. The physical conditions on both symmetrical surfaces are assumed to be the same. The ambient space outside the porous medium is included in the model to study the behavior of air flow at the outlet. The three dimensional mesh of the flat round porous aerostatic bearing with 2.6 million elements is shown in Fig. 3. Fig. 4 shows the sectional view of the mesh with 6 upward protrusions representing the air grooves and the extension representing the ambient space outside the porous material.

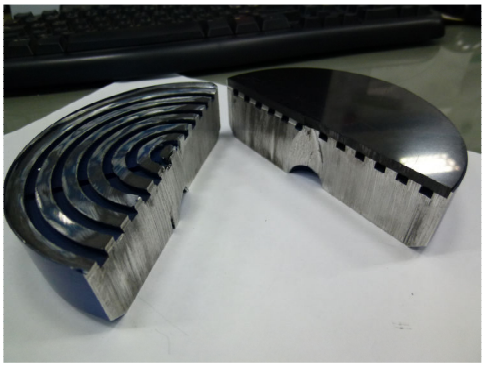

Fig. 1 A sectional view of the flat round porous aerostatic bearing

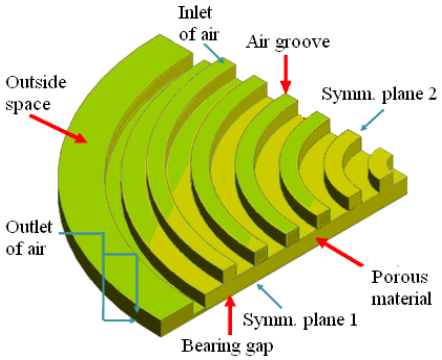

Fig. 2 The three dimensional geometric model of the bearing

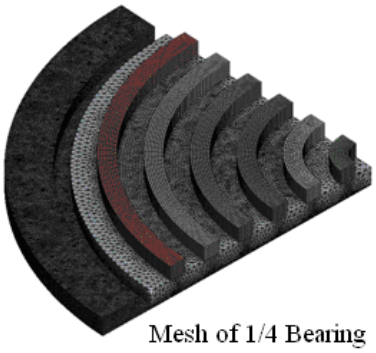

Fig.3 The three dimensional mesh of a quarter of the bearing

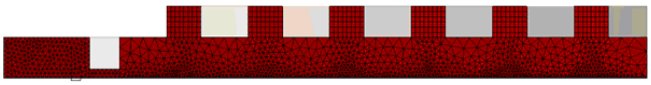

Fig. 4 The cross section of the mesh of the bearing

To analyze the steady state characteristics of the bearing and to simplify the calculation of the flow field, the velocity of the fluid on the solid surface is assumed to be zero due to non-slip condition. It is assumed that the air flow is laminar and isotropic inside the porous material. In addition, the pressure is assumed uniformly distributed over the air passages in the bearing housing. Based on the volume flow rate provided by the product catalog of the New Way Inc., the magnitude of flow resistance of the porous material can be figured out. The viscous resistance and the inertia resistance are assumed isotropic and at the values of 1.195×10^{14} and 1.975×10^{11},

respectively.

Five different porosity ratios, namely 0.05, 0.1, 0.2, 0.3 and 0.5, were assigned to each model of the porous material aerostatic bearing. The magnitude of the gap between the bearing and the guideway was considered as 5, 8, 10, 15 and 20 μm respectively. With a certain porosity ratio, in each steady state analysis, only one specific gap magnitude was considered in calculation of the pressure distribution in the gap. Finally, the variations of the pressure on the surface of the porous medium next to the air gap, which is named gap pressure in the paper, versus the magnitude of the gap were plotted for different porosity ratios to understand how the bearing load capacity varied with the bearing gap.

Based on the Navier-Stokes equation, the laminar flow module in FLUENT software was selected for simulating the characteristics of the bearing. The k-ε equation for turbulence was used to perform the steady state analysis of physical parameters. The second order Upwind Differentiating Technique was adopted to solve the heat convection terms. The SIMPLEC approach was applied to solve the iterative equations to get the velocity and the pressure. The convergent tolerance was assigned as 10^{-5}.

IV. Results and Discussion

The calculated results and the test data (from the New Way product specifications) of the average gap pressure (i.e., the pressure on the surface of the porous medium next to the air gap) are plotted in Fig. 5, which shows how the gap pressure varies with the gap thickness and the porosity of the porous material. The total load capacity of the bearing is figured out by multiplying the calculated average gap pressure by the surface area of the porous material. The average load capacity is defined as the load capacity per unit surface area of the porous material. Thus, the average load capacity is essentially the average gap pressure of the bearing. From the calculated results, it is known the average gap pressure of the bearing is 256.79kPa as the gap between the bearing and the guideway is 5μm and the porosity is 0.1. Multiplied it by the surface area of the porous material, which is 11882mm^2, the total load capacity can be figured out as 3051N. With the same gap and a porosity of 0.2, the average gap pressure is 226.15kPa and the total load capacity is 2687 N.

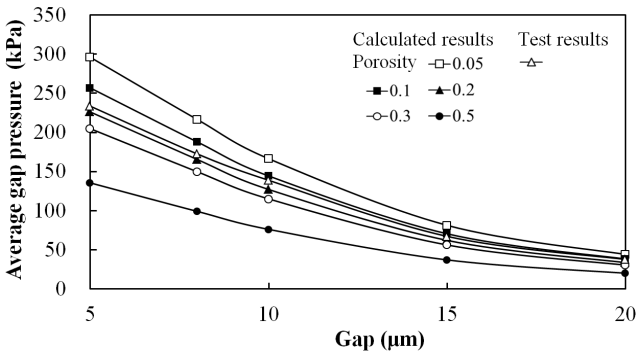

Fig. 5 Variation of the average gap pressure of the bearing versus the gap and the porosity

Fig. 6 shows, as the gap was 5μm and the porosity was unknown, the total load capacity of the type S1012501 bearing illustrated in the New Way product specifications is about 2775 N. Dividing it by the surface area of the porous material, which is 11882mm^2, the average load capacity was figured out as 233.54kPa. With a gap of 5μm, the percent difference between the computed result and the catalog datum is 9.9% for a porosity of 0.1. That value is -3.2% for a porosity of 0.2.

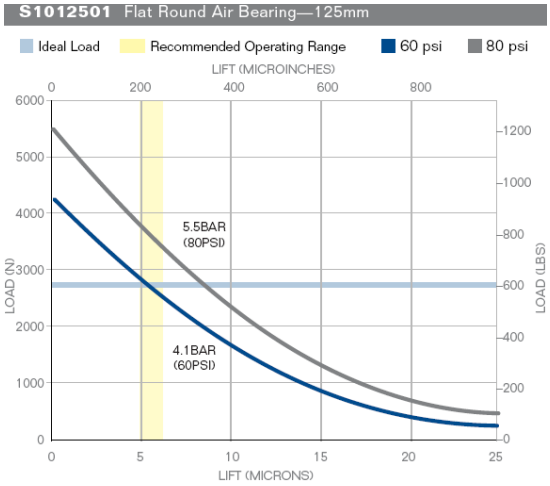

Fig. 6 The load capacity of the type S1012501 flat round porous aerostatic bearing varies with the gap. (Courtesy to New Way Inc.)

As the porosity is 0.1 and the gap is increased from 5μm to 20μm, the percent difference between the calculated average load capacity and the test result decreases from 9.9% to 1.4%. The calculated results constitute the upper bound of the test results. As the porosity is 0.2 and the gap is increased from 5 μm to 20μm, the percent difference increases from -3.2% to -10.7%. The calculated results constitute the lower bound of the test results. As the porosity is less than 0.1 or more than 0.2, the percent differences between the computed and the tested results are all larger. It indicates that the unknown porosity of the porous material of the type S1012501 bearing is possibly between 0.1 and 0.2.

In order to verify the analytical results, an experiment has been conducted by employing the mercury porosimetry technique to find out the realistic porosity. The porosity of the porous material is characterized by applying various levels of pressure to a piece of sample material immersed in mercury. The pressure required to intrude mercury into the sample's pores is inversely proportional to the size of the pores. The test results indicate the porosity is about 0.17. Thus, the adequacy of the simulation approach and the accuracy of the numerical results are confirmed.

Fig. 7 shows the pressure distribution on the cross sectional area of the porous material with a groove depth of 1mm, 2mm and 3.5mm, respectively. Clearly, it is seen that the change of groove depth does not vary the pressure distribution in the porous material. The load capacity of the bearing is not affected by the groove depth. In the steady state, the pressure in the groove is uniformly distributed. The effect of the geometry of

the inlet on the pressure can be ignored. That is the reason the inlet is simplified in the model as shown in Fig. 2.

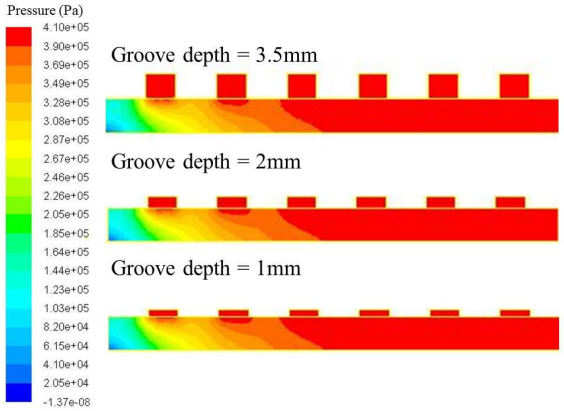

Fig. 7 The pressure distributed over the cross section of the porous material of the bearing with a groove depth of 1mm, 2mm and 3.5mm, respectively

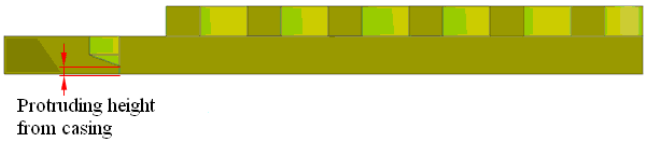

(a) Protruding height

(b) Edge chamfer

Fig. 8 The cross section of bearing shows the geometric parameters

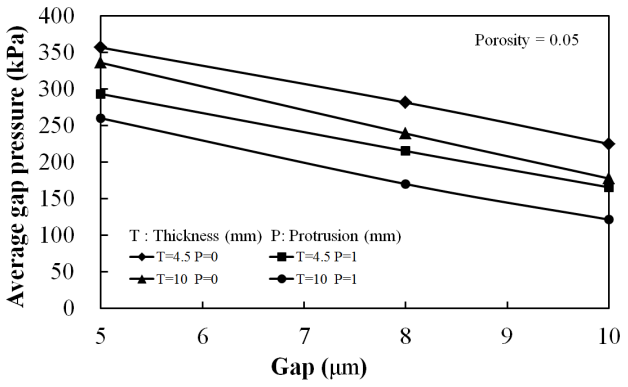

(a)

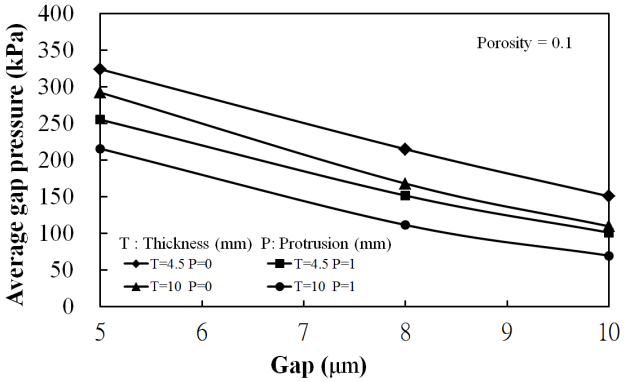

(b)

Fig. 9 The effects of air gap, porosity, thickness and protruding height of the porous material on the average load capacity of the bearing

With a protruding height of 1mm from the aluminum housing (Fig. 8 (a)), the overall thickness of the porous material of type S1012501 bearing is 4.5 mm. The effects of the air gap, the porosity, the thickness and the protruding height of the porous material on the average load capacity of the bearing are illustrated in Fig. 9. It is observed in Fig. 9 (a), as the porosity is 0.05, the thickness of the porous material is 4.5mm and there is no protrusion, the average load capacity per unit area of the bearing is the largest. When the thickness of the porous material or the protruding height increases, the gap pressure will decrease. So does the average load capacity. When the thickness of the porous material decreases, the pressure gradient at both sides of the cross section of the bearing becomes less steep. Therefore, the smaller the protruding height, the larger the average load capacity. However, the porous material cannot be too thin. Otherwise, the stiffness of the bearing will be insufficient.

If the porosity is 0.05 and the chamfer angle at the edge of the bearing is zero or 20 degrees (Fig. 8 (b)), the variation of the average load capacity of the bearing versus the bearing gap is shown in Fig. 10. The calculated results show, as the chamfer angle is increased from zero to 60 degrees, the change in average load capacity is less than 0.1%. In engineering, such a slight change is negligible. It indicates that the change in the chamfer angle does not substantially vary the gap pressure and the load capacity of the bearing.

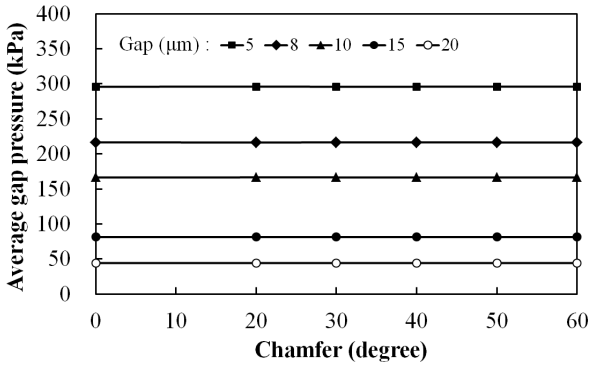

Fig. 10 The effects of chamfer angle and air gap on the average load capacity of the bearing

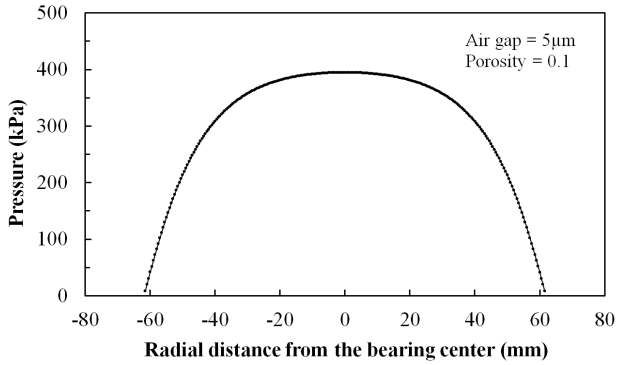

Fig. 11 The pressure distribution on the surface of the porous material varies with the radial distance from the center of the bearing moving at a constant speed of 1m/s

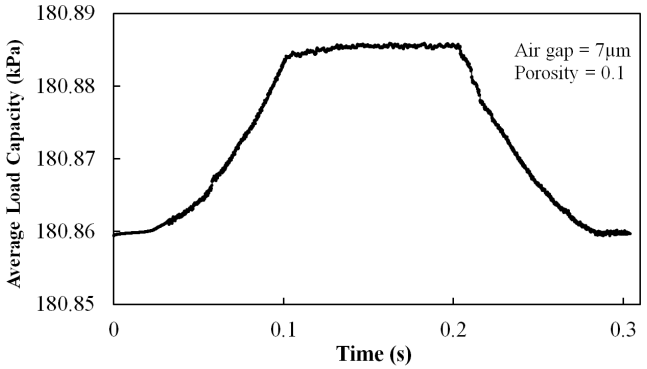

Fig. 12 The average load capacity of the bearing changes with the time varying moving speed

When the bearing with a porosity of 0.1 and a gap of 5μm is stationary or moving linearly at a constant speed of 1m/s or 2 m/s, the average load capacity is figured out to be 256.79kPa, 255.58kPa and 256.05kPa, respectively. It is found, with a small bearing gap such as 5μm, the load capacity of the bearing is almost not affected if its moving speed is changed. Fig. 11 shows the pressure distribution in radial directions on the surface of the porous material of the bearing which is moving at a constant speed of 1m/s. As the bearing moves at a constant speed of 2m/s, the pressure distribution is basically in the same shape and value as those shown in Fig. 11.

As the porosity is 0.1 and the bearing gap is 5μm, 7μm and 10μm respectively, the average load capacities of the bearing at different time and moving velocities were calculated. The time varying velocity $v(t)$ is defined as: $0 \le t < 0.1$ s, $v = at$ m/s; 0.1 s $\le t \le$ 0.2 s, v = 1m/s; 0.2 s $< t \le$ 0.3 s, $v = 1\text{-}a(t\text{-}0.2)$ m/s, where the acceleration a is 10m/s^2. It is found, when the gap is as small as 5μm, no matter the bearing accelerates, moves at constant speed or decelerates, the load capacity of the bearing changes very slightly (less than 1.1Pa). The effect of the change of speed on the load capacity of the bearing is insignificant. The gap pressure distribution is not affected by acceleration and deceleration of the linear movement of the bearing. No matter at what time and speed, the distribution of gap pressure at radial locations on the cross section of the bearing is the same as that shown in Fig. 11. Due to large computation in a transient analysis, it takes about 8 days to complete each run. With a gap of 7μm and a porosity of 0.1, the variations of the bearing velocity and the gap pressure versus time are shown in Fig. 12. It illustrates that as the bearing accelerates, its average load capacity increases; as the bearing decelerates, the average load capacity decreases.

It is noticed that, with the same porosity and the time varying velocity, if the gap is increased from 5μm to 10μm, the maximum difference in the average load capacity of the bearing increases from 1Pa to 47Pa. It indicates that, when the gap is increased, the change in the moving speed of the bearing influences its load capacity more.

If the bearing gap is unchanged, the faster the speed of the bearing, the higher the hydrodynamic pressure and the load capacity of the bearing will be. It is found that, when the bearings move at the same time varying speed, the one with larger gap will gain the hydrodynamic pressure and the load capacity in a higher percentage as its speed is increased. However, for the bearing with larger gap, its hydrostatic pressure loses even more. In consequence, the total load capacity of the bearing with larger gap is lower than the one with smaller gap.

V. Conclusion

The accuracy in measurement of the porosity of the porous material depends on the testing facility, the equipment and the method. It is often questionable. Since the porosity of the S1012501 type flat round porous aerostatic bearing made by New Way is not listed in its product specifications, the porosity was assumed for the porous material in analysis of the gap pressure and load capacity of the bearing. From the analytical results, it is estimated that the unknown porosity of the porous material is possibly between 0.1 and 0.2. The experimental results show the porosity is about 0.17. It confirms the validity of the numerical model and the simulation approach used in this study.

From the parametric study, it is understood that the depth of the air groove and the edge chamfer do not influence the gap pressure and the load capacity of the bearing. When the thickness of the porous material or the protruding height increases, the bearing gap pressure will decrease. Also, the smaller the protruding height or the thickness of the porous material is, the larger the average load capacity will be. But the porous material can't be too thin to assure sufficient stiffness of the bearing.

When the bearing gap is as small as 5μm, the variation in the translational velocity of the bearing affects its load capacity and the distribution of the gap pressure very insignificantly. For the

bearing with a larger gap, the increase in the moving speed will result in a minor gain in dynamic pressure. However, the static pressure of the bearing loses even more. In consequence, the total load capacity of the bearing with larger gap is lower than the one with smaller gap. The study verifies the fact that the larger the porosity, the worse the average load capacity per unit surface area of the porous medium.

ACKNOWLEDGMENT

The authors are grateful to the Industrial Technology Research Institute of the ROC, for the financial support of this research under grant No. B352A32240.

REFERENCES

[1] S. A. Sheinberg, and V. G. Shuster, "Resistance to vibration of a hydrostatic thrust bearing," *Mach. Tooling*, vol. 31 no. 11, pp. 24–29, Nov. 1960.
[2] E. P. Gargiulo, Jr., and P. W. Gilmour, "A numerical solution for the design of externally pressurized porous gas bearings: thrust bearings," *Trans. ASME, J. Tribol.*, vol. 90, no. 4, pp. 810–817, Oct. 1968.
[3] A. Andrisano, and A. Maggiore, "Theoretical and experimental analysis of an externally pressurized porous gas thrust bearing," *Tribol. Int.*, vol. 11, no. 5, pp. 285–288, Oct. 1978.
[4] S. Ishizawa, and E. Hori, "The flow of viscous fluid through a porous wall into a narrow gap-a consideration of the slip of fluid on a porous surface," *Bull.*, *JSME*, vol. 9, no. 36, pp. 719–730, Nov. 1966.
[5] G. S. Beavers, and D. D. Joseph, "Boundary conditions at a naturally permeable wall," *J. Fluid Mech.*, vol. 30, no. 1, pp. 197–207, Oct. 1967.
[6] P. R. K. Murti, "Effect of velocity slip in an externally pressurized porous thrust bearing working with an incompressible fluid," *Trans. ASME, J. Appl. Mech.*, vol. 43, no. 3, pp. 404–408, Sep. 1976.
[7] R. L. Verma, "Effect of velocity slip in an externally pressurized porous circular thrust bearing," *Wear*, vol. 63, no. 2, pp. 239–244, Sep. 1980.
[8] F. C. Hsing, "The effect of fluid inertia on a porous thrust plate: An analytical solution," *Trans. ASME*, *J. Tribol*, vol. 93, no. 1, pp. 202–206, Jan. 1971.
[9] R. Taylor, and G. K. Lewis, "Steady-state solutions for an aerostatic thrust bearing with an elastic porous pad," in *Proc. 6th Int. Gas Bearing Symp.,* Mar. 1974, paper C5.
[10] N. S. Rao, "Analysis of aerostatic porous rectangular thrust bearings with offset loads," *Wear*, vol. 59, no. 2, pp. 333–344, Mar. 1980.
[11] N. S. Rao, "Effect of slip flow in aerostatic porous rectangular thrust bearings," *Wear*, vol. 61, no. 1, pp. 77–86, Jun. 1980.
[12] K. C. Singh, and N. S. Rao, "Analysis of aerostatic porous annular thrust bearings with tilt," *Wear*, vol. 80, no. 3, pp. 291–299, Sep. 1982.
[13] K. C. Singh, and N. S. Rao, "Static characteristics of aerostatic porous rectangular thrust bearings with offset load," *Trans. ASME*, *J. Lubr. Technol.*, vol. 105, no. 1, pp. 143–146, Jan. 1983.
[14] K. C. Singh, and N. S. Rao, "Static axial characteristics of aerostatic annular porous thrust bearings with tilt," *Proc. I MechE Part C: Mech. Eng. Sci.*, vol. 197, pp. 83–88, Apr. 1983.
[15] K. C. Singh, N. S. Rao, and B. C. Majumdar, "Effect of velocity slip on the performance of aerostatic porous thrust bearings with uniform film thickness," *Wear*, vol. 88, no. 3, pp. 323–333, Jul. 1983.
[16] K. C. Singh, N. S. Rao, and B. C. Majumdar, "Steady-state characteristics of aerostatic porous rectangular thrust bearings incorporating the effects of velocity slip, anisotropy and tilt," *Proc. I MechE Part C: Mech. Eng. Sci.*, vol. 197, pp. 179–188, Sep. 1983.
[17] K. C. Singh, N. S. Rao, and B. C. Majumdar, "Effects of velocity slip, anisotropy and tilt on the steady state performance of aerostatic porous annular thrust bearings," *Wear*, vol. 97, no. 1, pp. 51–63, Aug. 1984.
[18] T. Koyama, T. Aoyama, and I. Inasaki, "Characteristics of externally pressurized porous ceramics air bearings," *Trans. JSME, Part C*, vol. 55, pp. 750–757, Mar. 1989.
[19] Y. Tian, "Static study of the porous bearings by the simplified finite element analysis," *Wear*, vol. 218, no. 2, pp. 203–209, Jul. 1998.
[20] Y. B. P. Kwan, and J. Corbett, "A Simplified method for the correction of velocity slip and inertia effects in porous aerostatic thrust bearings," *Tribol. Int.*, vol. 31, no. 12, pp. 779–786, Dec. 1998.
[21] S. Yoshimoto, and K. Kohno, "Static and dynamic characteristics of aerostatic circular porous thrust bearings (effect of the shape of the air supply area)," *Trans. ASME*, *J. Tribol.*, vol. 123, no. 3, pp. 501–508, Jul. 2001.
[22] T. S. Luong, W. Potze, J. B. Post, R. A. J. van Ostayen, and A. van Beek, "Numerical and experimental analysis of aerostatic thrust bearings with porous restrictors," *Tribol. Int.*, vol. 37, no. 10, pp. 825–832, Oct. 2004.
[23] M. Miyatake, S. Yoshimoto, and K. Yagi, "Static and dynamic characteristic of aerostatic porous thrust bearings with deep feed groove," *Trans. JSME, Part C*, vol. 71, no. 2, pp. 738–744, Feb. 2005.
[24] D. Z. Wu, and J. Z. Tao, "Analysis on the static performance of porous graphite aerostatic thrust bearings*,"* in *2010 Proc. Int. Conf. Comput. Eng. Technol*., vol. 5, pp. V5112-5115.
[25] B. E. Launder, and D. B. Spalding, *Lectures in mathematical models of turbulence*, London: Academic Press, 1972.
[26] J. O. Hinze, *Turbulence*, New York: McGraw-Hill, 1975.